Available online at www.sciencedirect.com

ScienceDirect

IFAC PapersOnline CONFERENCE PAPER ARCHIVE

IFAC PapersOnLine 56-2 (2023) 4484–4489

# Backstepping Control of a Motorized Ankle Orthosis Targeting the Soleus Muscle During Walking*

**Nicholas Rubino**[1], **Eleanor Lawler**[1], **Jonathan Casas**[1], **Victor H. Duenas**[1]

[1] *Department of Mechanical and Aerospace Engineering, Syracuse University, 13244 NY, USA.(e-mail:{narubino, ejlawler, jacasasb, vhduenas}@syr.edu).*

**Abstract:** The gait patterns of stroke survivors become slow and metabolically inefficient as a result of muscle weakness and low weight-bearing capacity. Exoskeletons and assistive robots can improve gait kinematics and energetics. However, the use of these powered devices may cause a reliance on the device itself that results in limited lasting improvement of the paretic leg function. Specifically, there exists a need to strengthen and train the response of weak ankle muscles, such as the soleus muscle, in stroke survivors. Impaired activation of the soleus muscle induces unnatural gait kinematics and reduced propulsion. The mechanical modulation of the soleus muscle can improve its loading response and enhance gait performance after a stroke. This paper develops a closed-loop feedback controller to manipulate the ankle joint dynamics to mechanically control the soleus muscle response using a motorized ankle orthosis. The control method is inspired by backstepping control techniques and developed to connect the ankle joint angular velocity and the soleus muscle response during the stance phase of walking. The tracking objective is quantified using an integral-like muscle error between the desired soleus response and the actual muscle response, which is measurable using surface electromyography (EMG). The closed-loop electric motor controller is designed to apply ankle perturbations exploiting the backstepping error and an adaptive control term to cope with uncertain parameters that satisfy the linear-in-the-parameters property. A switching signal is developed using heel and toe ground reaction forces to strategically perturb the ankle and target the soleus muscle loading response in real-time during the mid-late stance phase of walking. A Lyapunov-based stability analysis is used to guarantee a globally uniformly ultimately bounded (GUUB) tracking result.



*Keywords:* Backstepping, Lyapunov methods, Robust control, Walking devices

## 1. INTRODUCTION

Stroke survivors experience impairments that negatively affect gait function. Secondary conditions post-stroke include muscle weakness, low weight-bearing capacity, and loss of balance, which all contribute to the consistent partial disuse of the paretic leg (Weerdesteyn et al., 2008). Over time, these conditions yield unnatural, slow and metabolically inefficient gait patterns. Thus, there exists a need to develop methods for restoring gait function in people post-stroke. The use of robotic-assistive devices for gait rehabilitation can improve gait kinematics and energetics (Marchal-Crespo and Reinkensmeyer, 2009). However, the lasting benefits of assistive rehabilitation devices have been marginal. Robotic exoskeletons can induce a reliance on such assistive devices in the individuals for whom they are built (Hornby et al., 2020). For instance, an assistive device may enhance paretic leg function during isolated gait sessions; however, there is a gap in knowledge on how to guarantee functional benefits are retained during the long-term recovery process after a stroke. Thus, there exists a need to develop systematic human-robot control methods for training in which people post-stroke undergo muscle conditioning facilitated by wearable devices. Such paradigms hold the potential to yield lasting functional improvements as the wearable devices are only used during training. In particular, motivation exists to improve walking by inducing improvements in the muscle activation patterns of stroke survivors.

The ankle joint and soleus muscle are critical during natural walking (Kulmala et al., 2016; Lipfert et al., 2014). The ankle joint-soleus muscle system is essential in providing energy for balance control and propulsion in the stance phase of walking (Winter, 2009). After a stroke,

*Research reported in this publication was supported in part by the National Science Foundation under Grant No. 2218913 and by pilot funding from the National Institutes of Health National Center of Neuromodulation for Rehabilitation, the National Center for Complementary and Integrative Health, the National Institute on Deafness and Other Communication Disorders, and the National Institute of Neurological Disorders and Stroke; NIH/NICHD Grant Number P2CHD086844 which was awarded to the Medical University of South Carolina. The contents are solely the responsibility of the authors and do not necessarily represent the official views of the NSF, NIH or NICHD.


10.1016/j.ifacol.2023.10.938

the propulsive force, balance, and muscle activation of the ankle joint-soleus muscle system is diminished. Thus, there exists motivation to develop a training paradigm capable of strengthening the ankle joint and soleus muscle of stroke survivors. In particular, mechanically manipulating the ankle joint can yield increments in soleus muscle activity (Mazzaro et al., 2005). Hence, a critical need is to design controllers for wearable devices that can adapt the responses of muscles during human training strategies. This implies developing controllers that fundamentally depart from assistive exoskeletons and neuromuscular electrical stimulation that track natural gait patterns during rehabilitative strategies (Gandolla et al., 2018). An outstanding technical challenge is to develop closed-loop control approaches during real-time walking for targeting the soleus muscle, since existing work has primarily developed open-loop or proportional-derivative control approaches (Andersen and Sinkjaer, 1995; Mazzaro et al., 2005). Open-loop control approaches at the clinic fail to adapt and compensate for the change in muscular responses in real-time. Thus, a robust closed-loop control method is well-motivated to evoke reliable muscle responses during human conditioning and training, which can induce lasting functional benefits after a stroke independent of the assistance of an exoskeleton or robot.

Developing non-invasive strategies to mechanically control muscle function in individual's post-stroke during real-time walking is challenging. Specifically, there is an uncertain mapping between the joint dynamics and the muscle responses throughout the step cycle. Additionally, the muscular system dynamics have parametric and functional uncertainties that exacerbates the difficulty to predict muscle responses and reliably quantify performance (Perreault et al., 2000). Thus, the strategy in this paper is to develop a closed-loop feedback controller that can exploit the soleus muscle responses using surface electromyography (EMG) to mechanically manipulate the ankle joint through the control of a wearable device.

A backstepping control approach (or integrator backstepping (Krstić et al., 1995)) can be used to link the cascaded dynamics of the ankle joint and the soleus muscle responses through the design of a backstepping error and a virtual controller. However, it is unclear how to compensate for the uncertainty in the overall system including the wearable robot, ankle dynamics and muscle responses. In addition, there are fundamental challenges and limitations in the design of the backstepping error and virtual controller including the need to compensate for the cascaded uncertainty and to mitigate the explosion of terms when computing high-order derivatives. The development of closed-loop feedback controllers for the ankle to modulate the soleus response specifically during walking remains limited due to the technical control challenges.

In this paper, a closed-loop feedback controller is designed to evoke desired soleus muscle responses within the mid-late stance phase of walking using a motorized ankle-foot orthosis. The ankle joint dynamics are modeled as a Euler-Lagrange system with viscous and elastic effects, and the soleus muscle response within the stance phase is modeled based on the ankle joint angular velocity (Gottlieb and Agarwal, 1979; Yang et al., 1991). To design the electric motor controller to evoke the desired muscle responses, an integral-like muscle error and a backstepping control approach are developed to interconnect the joint velocity and muscle output. Thus, the backstepping approach injects a virtual control input to influence the soleus muscle response through the ankle angular velocity. The designed motor controller exploits the backstepping error, robust terms to compensate for state-dependent uncertainty, and an adaptive control term to estimate the system's constant inertial and viscous damping parameters, which appear linearly in the closed-loop dynamics. The adaptive update law exploits a projection algorithm to ensure bounded adaptive estimation errors. A piecewise continuous switching signal is developed to activate the motor controller only within the stance phase using ground reaction forces of the heel and toe, and the soleus muscle response is measured using EMG. A Lyapunov-based stability analysis is developed to ensure globally uniformly ultimately bounded (GUUB) tracking of the soleus muscle response within the perturbation region.

## 2. DYNAMIC MODEL

### *2.1 Ankle Joint Dynamic Model*

The single degree-of-freedom ankle-joint muscle-tendon system and a powered ankle-foot orthosis is modeled with the following Euler-Lagrange dynamics

$$\tau_r(\dot{q},\ddot{q}) + \tau_a(q,\dot{q},\ddot{q}) + G(q) = \tau_e(t), \tag{1}$$

where $q : \mathbb{R}_{\geq t_0} \to \mathcal{Q}$ denotes the measurable ankle joint angular position, $\mathcal{Q} \subset \mathbb{R}$ denotes the set of ankle joint angles, and $t_0 \in \mathbb{R}$ is the initial time; $\dot{q}, \ddot{q} : \mathbb{R}_{\geq t_0} \to \mathbb{R}$ denote the measurable angular velocity and unmeasurable angular acceleration, respectively; $G(q) : \mathcal{Q} \to \mathbb{R}$ denotes the effects of gravity and is defined as $G \triangleq mgl\sin(q)$, where $m \in \mathbb{R}_{>0}$ is the combined mass of the foot and orthosis, $g \in \mathbb{R}$ is the acceleration due to gravity, and $l \in \mathbb{R}_{>0}$ is the distance between the ankle-joint and the lumped center of the mass of the ankle-foot-orthosis; and the net robotic orthosis torque denoted by $\tau_r : \mathbb{R}^2 \to \mathbb{R}$ and the ankle-joint muscle-tendon torque, i.e., the passive, intrinsic dynamics (Perreault et al., 2000), denoted by $\tau_a : \mathcal{Q} \times \mathbb{R}^2 \to \mathbb{R}$ are defined as

$$\tau_r(\dot{q},\ddot{q}) \triangleq J_r\ddot{q} + b_r\dot{q}, \tag{2}$$

$$\tau_a(q,\dot{q},\ddot{q}) \triangleq I\ddot{q} + P(q,\dot{q}), \tag{3}$$

where $J_r \in \mathbb{R}_{>0}$ is an uncertain positive constant denoting the inertia of the powered ankle-foot-orthosis, $b_r \in \mathbb{R}$ is an uncertain positive constant denoting the viscous damping effects of the robotic device (Andersen and Sinkjaer, 1995), $I \in \mathbb{R}_{>0}$ is an uncertain positive constant denoting the inertia of the ankle joint tendon-muscle system, $P(q,\dot{q}) : \mathcal{Q} \times \mathbb{R} \to \mathbb{R}$ denotes the viscous effects due to damping in the musculotendon complex and elasticity due to ankle stiffness and is defined as $P \triangleq K_1\exp(-K_2 q)(q - K_3) - B_1\tanh(-B_2\dot{q}) + B_3\dot{q}$, where $K_1, K_2, K_3, B_1, B_2, B_3 \in \mathbb{R}_{>0}$ are uncertain positive constants as described in (Downey et al., 2017), (Schauer et al., 2005), and (Riener et al., 2000).

The torque applied by the electric motor about the ankle joint denoted by $\tau_e : \mathbb{R}_{\geq t_0} \to \mathbb{R}$ can be defined as

$$\tau_e(t) \triangleq B_e\sigma_p u_e(t), \tag{4}$$

where $u_e : \mathbb{R}_{\geq t_0} \to \mathbb{R}$ is the subsequently designed motor current control input, $\sigma_p \in \{0, 1\}$ is the switching signal developed in the next subsection, and $B_e \in \mathbb{R}_{>0}$ is the known positive torque constant.

### *2.2 Switching System and Soleus Muscle Models*

In this section, the ankle-joint dynamic model in (1) is further developed to account for switching the electric motor to apply the ankle joint perturbation to induce a soleus muscle loading response. The electric motor is activated only within the mid-late stance phase of walking to target the soleus muscle. A piecewise constant switching signal denoted by $\sigma_p$ is developed to apply an ankle joint perturbation per step cycle and is defined as

$$\sigma_p(t) \triangleq \begin{cases} 1, & t \in \mathcal{T} \\ 0, & t \notin \mathcal{T} \end{cases}, \tag{5}$$

where $\mathcal{T}$ is the perturbation region within the step cycle defined as

$$\mathcal{T} \triangleq \{t \in \mathbb{R}_{\geq t_0} \mid (x_1(t) \geq \underline{x}) \wedge (x_2(t) \geq \overline{x})\}, \tag{6}$$

where $x_1, x_2 : \mathbb{R}_{\geq t_0} \to \mathbb{R}_{>0}$ are measurable heel and toe ground reaction forces, and $\underline{x}, \overline{x} \in \mathbb{R}_{>0}$ denote the prescribed lower and upper thresholds of ground reaction forces, respectively, that uniquely define the mid-late stance phase of walking. The lower force threshold determines the instance to start applying the ankle joint perturbation to adequately target the soleus muscle response. The upper force threshold determines the instance to stop the perturbation to prevent interfering with the swing phase of walking. A gait detection algorithm is developed to monitor the gait phases denoted as $\mathcal{S} = \{SW, HS, PR, SP\}$, where $SW$ denotes the swing phase, $HS$ denotes the heel strike, $PR$ refers to the perturbation region, and $SP$ denotes the phase at which the perturbation is stopped. The force thresholds defined in (6), ensure that the ankle perturbation only occurs during the mid-late stance phase of walking, i.e., $\mathcal{S} = \{PR\}$; thus, the electric motor is turned off outside of the perturbation region. The dynamic model in (1) can be rearranged by substituting (2)-(4) into (1) and exploiting (5) to yield

$$M\ddot{q} + P(q, \dot{q}) + G(q) + b_r\dot{q} + d(t) = B_e\sigma_p u_e(t), \tag{7}$$

where $M \in \mathbb{R}_{>0}$ denotes the combined inertial effects of the overall system and is defined as $M \triangleq J_r + I$; and $d : \mathbb{R}_{\geq t_0} \to \mathbb{R}$ denotes the external exogenous disturbances including unmodeled effects in the musculoskeletal system.

Leveraging the results in (Gottlieb and Agarwal, 1979) and (Yang et al., 1991), the soleus muscle response can be modeled as a state-dependent system on the ankle joint angular velocity as

$$S = s_1 + s_2\dot{q}(t), \tag{8}$$

where $S : \mathbb{R} \to \mathbb{R}$ is the measurable EMG of the soleus response due to the applied ankle joint rotation within the perturbation region and $s_1, s_2 \in \mathbb{R}_{>0}$ are uncertain positive constants. The implementable soleus muscle response is obtained as

$$S = S_m - S_b, \tag{9}$$

where $S_b : \mathbb{R}_{\geq t_0} \to \mathbb{R}$ denotes baseline EMG recorded during unperturbed step cycles and $S_m : \mathbb{R}_{\geq t_0} \to \mathbb{R}$ denotes the real-time soleus EMG measurements. Figure 1 shows the block diagram illustrating the closed-loop control system for the powered orthosis and ankle-joint dynamics with soleus muscle EMG feedback.

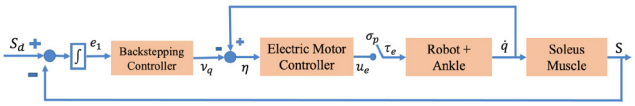


Fig. 1. Block diagram of the closed-loop feedback system integrating a powered ankle-foot orthosis and the ankle-joint system. The soleus muscle response is formulated leveraging the results in (Yang et al., 1991) and (Gottlieb and Agarwal, 1979).

The following properties and assumptions are exploited in the subsequent control design and stability analysis.

*Property 1.* $c_m \leq M \leq c_M$, where $c_m, c_M \in \mathbb{R}_{>0}$ are known constants.

*Property 2.* $|P(q, \dot{q})| \leq c_{p1} + c_{p2}|\dot{q}|$, where $c_{p1}, c_{p2} \in \mathbb{R}_{>0}$ are known constants.

*Property 3.* $|G(q)| \leq c_g$, where $c_g \in \mathbb{R}_{>0}$ is a known constant.

*Assumption 1.* The exogenous disturbance $d$ is upper bounded as $|d| \leq \zeta_d$, where $\zeta_d \in \mathbb{R}_{>0}$ is a known constant.

*Assumption 2.* The desired EMG response $S_d \in \mathbb{R}$ is designed as continuous, bounded function such that $|S_d| \leq \overline{s_d} \in \mathbb{R}_{>0}$.

## 3. CONTROL DEVELOPMENT

The control objective is to design a motor controller that induces changes in soleus EMG $S(t)$ due to applying kinematic perturbations about the ankle joint. To interconnect the dynamics in (7) and the soleus muscle response in (8), a backstepping control approach is introduced to develop the electric motor controller $u_e$ to drive the soleus muscle dynamics to a desired EMG response through manipulation of the ankle joint angular velocity $\dot{q}$. To quantify the tracking objective, a measurable integral error signal $e_1 : \mathbb{R}_{\geq t_0} \to \mathbb{R}$ is defined as

$$e_1 \triangleq \int_{t_p}^{t} (S_d(\varphi) - S(\varphi))\, d\varphi, \tag{10}$$

where $S_d \in \mathbb{R}_{>0}$ is the desired soleus EMG response due to the mechanical joint rotation of the ankle and $t_p \in \mathbb{R}_{\geq 0}$ is the time at which the perturbation begins to be applied at the start of the mid-late stance. The error is computed within the mid-late stance phase where the perturbation is applied, i.e., $\sigma_p = 1$. Taking the time derivative of (10), setting the initial conditions $S_d(t_p) = S(t_p)$ since a perturbation has not been applied yet (i.e., the desired EMG response is set to the current soleus EMG at the beginning of the perturbation region), and substituting (8) yields the open-loop error system

$$\dot{e}_1 = S_d - (s_1 + s_2\dot{q}). \tag{11}$$

To connect the soleus EMG response and the joint angular velocity, the backstepping error $\eta : \mathbb{R}_{\geq t_0} \to \mathbb{R}$ is defined as

$$\eta \triangleq \dot{q} - \nu_q, \tag{12}$$

where $\nu_q : \mathbb{R}_{\geq t_0} \to \mathbb{R}$ is a virtual controller. Substituting the virtual controller into (11) and performing algebraic manipulation yields

$$\dot{e}_1 = S_d - s_1 - s_2\eta - s_2\nu_q. \tag{13}$$

The virtual controller $\nu_q$ is designed as

$$\nu_q = k_1 e_1 + \frac{\rho_1^2}{\epsilon_1} e_1, \tag{14}$$

where $k_1, \epsilon_1 \in \mathbb{R}_{>0}$ are selectable control gains and $\rho_1 \in \mathbb{R}_{>0}$ is a known positive constant. Substituting (14) into (13) yields

$$\dot{e}_1 = S_d - s_1 - s_2\eta - s_2\big(k_1 e_1 + \frac{\rho_1^2}{\epsilon_1} e_1\big). \tag{15}$$

After taking the time derivative of (12) and premultiplying it by $M$, and then performing some algebraic manipulation yields

$$M\dot{\eta} = B_e u_e + \chi + N_d + Y\theta + e_1, \tag{16}$$

where the auxiliary signals $\chi : \mathbb{R}_{\geq t_0} \to \mathbb{R}$ and $N_d : \mathbb{R}_{\geq t_0} \to \mathbb{R}$ are defined as

$$\chi \triangleq -P(q, \dot{q}) - c_{p1} - e_1, \tag{17}$$

$$N_d \triangleq -G(q) - d + c_{p1}. \tag{18}$$

Using Assumption 1 and Property 3, the auxiliary signal in (18) can be upperbounded by

$$|N_d| \leq \xi_d, \tag{19}$$

where $\xi_d \in \mathbb{R}_{>0}$ is a known positive constant. By using Property 2, an upperbound for (17) can be developed as

$$|\chi| \leq \rho_2 \|z\|, \tag{20}$$

such that $|\chi|$ is linear in $||z||$ and thus, $\rho_2 \in \mathbb{R}_{>0}$ is a known constant, and $z : \mathbb{R}_{\geq t_0} \to \mathbb{R}^2$ is defined as $z \triangleq [\dot{q}\ e_1]^T$. Exploiting the linear-in-the-parameters property for the terms in (7), the known regressor $Y : \mathbb{R}^2 \to \mathbb{R}^{1\times 2}$ and uncertain constant parameter vector $\theta \in \mathbb{R}^2$ are defined as

$$Y \triangleq [-\dot{\nu}_q, -\dot{q}], \theta \triangleq \begin{bmatrix} M \\ b_r \end{bmatrix}, \tag{21}$$

where $\dot{\nu}_q$ is the time derivative of (14), which is implementable. The parameter estimation error denoted as $\tilde{\theta} : \mathbb{R}_{\geq t_0} \to \mathbb{R}^2$ is defined as

$$\tilde{\theta} \triangleq \theta - \hat{\theta}, \tag{22}$$

where $\hat{\theta} : \mathbb{R}_{\geq t_0} \to \mathbb{R}^2$ are the adaptive estimates. The control input $u_e : \mathbb{R}_{\geq t_0} \to \mathbb{R}$ is designed as

$$u_e = -\frac{1}{B_e}\Big(k_2\eta + Y\hat{\theta} + k_3\rho_2\|z\|\text{sgn}(\eta) + \frac{k_4}{\epsilon_2}\eta\Big), \tag{23}$$

where $k_2, k_3, k_4 \in \mathbb{R}_{>0}$ are selectable constant control gains. Motivated by the subsequent stability analysis, the adaptive update law is designed as

$$\dot{\hat{\theta}} = \text{proj}(\Gamma Y^T \eta), \tag{24}$$

where proj$(\cdot)$ is a projection algorithm (Krstić et al., 1995, Appendix E) and $\Gamma \in \mathbb{R}^{2\times 2}$ is a selectable positive-definite diagonal matrix. The closed-loop error dynamics are obtained after substituting the controller in (23) into the open-loop error dynamics in (16) as

$$M\dot{\eta} = \chi + N_d + Y\tilde{\theta} + e_1 - k_2\eta - k_3\rho_2\|z\|\text{sgn}(\eta) - \frac{k_4}{\epsilon_2}\eta. \tag{25}$$

## 4. STABILITY ANALYSIS

The stability of the electric motor controller within the perturbation region during the mid-late stance phase of walking can be examined using the following theorem.

*Theorem 1.* The controller designed in (23) and adaptive update law in (24) achieve globally uniformly ultimately bounded (GUUB) tracking in the sense that

$$\|w(t)\| \leq \sqrt{\frac{\gamma_2}{\gamma_1}}\|w(t_p)\| e^{-\frac{\gamma_6}{2}(t-t_p)} + \sqrt{\frac{\gamma_5}{\gamma_1\gamma_6}}\big(1 - e^{-\frac{\gamma_6}{2}(t-t_p)}\big), \tag{26}$$

where $\gamma_1, \gamma_2\, \gamma_5, \gamma_6 \in \mathbb{R}_{>0}$ are constants defined as

$$\gamma_1 \triangleq \min\big(\frac{1}{2s_2}, c_m, \frac{1}{2}\lambda_{\min}\{\Gamma^{-1}\}\big),$$
$$\gamma_2 \triangleq \max\big(\frac{1}{2s_2}, c_M, \frac{1}{2}\lambda_{\max}\{\Gamma^{-1}\}\big),$$
$$\gamma_5 \triangleq \frac{\lambda_1\gamma_4}{\gamma_3} + \bar{\epsilon},$$
$$\gamma_6 \triangleq \frac{\lambda_1}{\gamma_3},$$

and $\lambda_{\min}, \lambda_{\max}$ denote the minimum and maximum eigenvalue of the matrix, respectively. Further, $\gamma_3, \gamma_4, \lambda_1, \bar{\epsilon} \in \mathbb{R}_{>0}$ are positive constants defined below.

**Proof.** Let $V : \mathbb{R}^4 \times \mathbb{R}_{\geq t_0} \to \mathbb{R}$ be a positive definite, radially unbounded, continuously differentiable Lyapunov function candidate defined as

$$V \triangleq \frac{1}{2s_2}e_1^2 + \frac{1}{2}M\eta^2 + \tilde{\theta}^T\Gamma^{-1}\tilde{\theta}. \tag{27}$$

The function in (27) satisfies the following inequalities

$$\begin{aligned} \gamma_1\|y\|^2 &\leq V(y,t) \leq \gamma_2\|y\|^2, \\ V(y,t) &\leq \gamma_3\|w\|^2 + \gamma_4, \end{aligned} \tag{28}$$

where $y \triangleq [w^T, \tilde{\theta}^T]^T$, $w \triangleq [e_1, \eta]^T$, and $\gamma_3, \gamma_4 \in \mathbb{R}_{>0}$ are known positive bounding constants. Let $y(t)$ be a Filippov solution to the differential inclusion $\dot{y} \in K[h](y)$, where $K[h](\cdot)$ is defined as in (Filippov, 1964), and $h$ is defined by using (15), (22), (24), and (25) as $h \triangleq [h_1\ h_2\ h_3]$, where

$$h_1 \triangleq S_d - s_1 - s_2\eta - s_2\big(k_1 e_1 + \frac{\rho_1^2}{\epsilon_1}e_1\big),$$
$$h_2 \triangleq \frac{1}{M}\{\chi + N_d + Y\tilde{\theta} + e_1 - k_2\eta - k_3\rho_2\|z\|\text{sgn}(\eta) - \frac{k_4}{\epsilon_2}\eta\},$$
$$h_3 \triangleq -\text{proj}(\Gamma Y^T\eta).$$

The control input in (23) has the signum function; hence, the time derivative of (27) exists almost everywhere (a.e.), i.e., for almost all $t$. Based on (Fischer et al., 2013, Lemma 1), $\dot{V}(y,t) \overset{a.e.}{\in} \dot{\tilde{V}}(y,t)$, where $\dot{\tilde{V}}$ is the generalized time derivative of (27) along the Filippov trajectories of $\dot{y} = h(y)$ and is defined in Fischer et al. (2013) as $\dot{\tilde{V}} \triangleq \bigcap_{\xi\in\partial V} \xi^T K\begin{bmatrix} \dot{e}_1 & \dot{\eta} & \dot{\tilde{\theta}}^T & 1 \end{bmatrix}^T (e_1,\ \eta,\ \tilde{\theta}^T,\ t)$, where $\partial V(y,t)$ is the generalized gradient of $V$ at $(y,t)$. Since $V(y,t)$ is continuously differentiable in $y$, $\partial V = \{\nabla V\}$, $\dot{\tilde{V}} \overset{a.e.}{\subset} [e_1,\ M\eta,\ \tilde{\theta}^T\Gamma^{-1}]K\begin{bmatrix} \dot{e}_1 & \dot{\eta} & \dot{\tilde{\theta}}^T \end{bmatrix}^T$. Therefore, after substituting (15) and (25), canceling common terms, the generalized time derivative of (27) can be expressed as

$$\dot{\tilde{V}} \overset{a.e.}{\subset} \frac{1}{s_2} e_1 (S_d - s_1 - s_2(k_1 e_1 + \frac{\rho_1^2}{\epsilon_1} e_1)) + \tilde{\theta}^T \Gamma^{-1} \dot{\tilde{\theta}} + \eta(\chi + N_d + Y\tilde{\theta} - k_2\eta - k_3\rho_2||z||K[\text{sgn}(\eta)] - \frac{k_4}{\epsilon_2}\eta), \quad (29)$$

where $K[sgn(\eta)] = SGN(\eta)$ such that $SGN(\eta) = 1$ if $\eta > 0$, $[-1, 1]$ if $\eta = 0$, and $-1$ if $\eta < 0$. Substituting the upperbounds obtained in (19) and (20), (24), and using Assumption 2, the previous expression can be upperbounded as

$$\dot{\tilde{V}} \overset{a.e.}{\leq} -k_1 e_1^2 - k_2\eta^2 + \rho_1|e_1| - \frac{\rho_1^2}{\epsilon_1} e_1^2 + \rho_2||z|||\eta| - k_3\rho_2||z|||\eta| + \eta\xi_d - \frac{\xi_d^2}{\epsilon_2}\eta^2, \quad (30)$$

where $\rho_1 = \frac{1}{s_2}(\overline{s_d} + \overline{s_1})$ is a positive bounding constant and $k_4 \triangleq \xi_d^2$. By selecting $k_3 > 1$ and if $\rho_1|e_1| < \epsilon_1$ and $\xi_d|\eta| < \epsilon_2$, the previous inequality can be further upper bounded as

$$\dot{\tilde{V}} \overset{a.e.}{\leq} -k_1 e_1^2 - k_2\eta^2 + \bar{\epsilon} \overset{a.e.}{\leq} -\lambda_1||w||^2 + \bar{\epsilon}, \quad (31)$$

where $\lambda_1 = \min(k_1, k_2)$ and $\bar{\epsilon} \triangleq \epsilon_1 + \epsilon_2$. Further by using the last inequality in (28), the inequality in (31) can be upperbounded as

$$\dot{\tilde{V}} \overset{a.e.}{\leq} -\gamma_6 V + \gamma_5, \quad (32)$$

where $\gamma_5 \triangleq \frac{\lambda_1\gamma_4}{\gamma_3} + \bar{\epsilon}$ and $\gamma_6 \triangleq \frac{\lambda_1}{\gamma_3}$. Applying the Comparison Lemma (H. K. Khalil, 2002, Lemma 3.4) to (32) yields

$$V(y) \overset{a.e.}{\leq} V(y(t_p))e^{-\gamma_6(t-t_p)} + \frac{\gamma_5}{\gamma_6}(1 - e^{-\gamma_6(t-t_p)}), \quad (33)$$

which can be used with the first two inequalities in (28) to yield the GUUB tracking result in (26). Using (27) and (33), $V \in \mathcal{L}_\infty$; hence, $e_1, \eta, \tilde{\theta} \in \mathcal{L}_\infty$, which implies that $\nu_q, \hat{\theta}, S \in \mathcal{L}_\infty$ and yields $\dot{q} \in \mathcal{L}_\infty$ in (12), and then $z \in \mathcal{L}_\infty$. Further, $\dot{e}_1 \in \mathcal{L}_\infty$, then $\dot{\nu}_q \in \mathcal{L}_\infty$, which implies that $Y \in \mathcal{L}_\infty$ and thus, $u_e \in \mathcal{L}_\infty$ in (23) resulting in $\tau_e \in \mathcal{L}_\infty$ in (4).

From (30), asymptotic tracking is achieved if $\rho_1|e_1| > \epsilon_1$ and $\xi_d|\eta| > \epsilon_2$ and by invoking (Fischer et al., 2013, Corollary 2), and since $\dot{\tilde{V}}(y,t) \overset{a.e.}{\leq} -W(y)$, thus $|e_1| \to 0$ as $t \to \infty$, where $W$ is a continuous positive semi-definite function.

The following lemma establishes a bound for $\dot{e}_1$ for all time.

*Lemma 1.* The soleus muscle error dynamics $\dot{e}_1$ in (15) is uniformly bounded within the perturbation region of the stance phase of walking in the sense that

$$|\dot{e}_1(t)| \leq s_2\Big(\rho_1\Big(1 + \Big(\frac{k_1}{\rho_1} + \frac{\rho_1}{\epsilon_1}\Big)e_1\Big) + \eta\Big). \quad (34)$$

**Proof.** The integral-like muscle error $e_1$ can be expressed as

$$e_1(t) = \int_{t_p}^{t} \frac{de_1(\varphi)}{d\varphi}\, d\varphi + c_1, \quad (35)$$

where $c_1 \in \mathbb{R}$ is an integration constant. Exploiting the inequality in (26) and (35), it can be established that $lim_{t\to\infty} \int_{t_p}^{t} \frac{de_1(\varphi)}{d\varphi}\, d\varphi$ exists and it is finite. Using (15) and (14), the upperbound in (34) can be obtained. Therefore, exploiting Theorem 1 to prove that $e_1, \eta \in \mathcal{L}_\infty$, then $\dot{e}_1 \in \mathcal{L}_\infty$.

## 5. CONCLUSION

An electric motor controller was designed and analyzed in this paper to evoke a soleus muscle response within the stance phase of walking. The prescribed desired soleus target response is tracked by the closed-loop feedback controller that activates the motor of a powered ankle orthosis. A backstepping control approach is developed to interconnect the ankle joint dynamics and the soleus muscle responses. The virtual controller exploits an integral-like muscle error and the motor controller exploits the backstepping error and an adaptive feedback term to compensate for the uncertain inertial and viscous damping parameters in the robot-ankle system. A Lyapunov-based stability analysis was developed to ensure a GUUB result due to the uncertainty in the parameters of the soleus muscle response. Future work includes implementing the controller in participants to characterize the sensitivity of the developed control method. In addition, future efforts involve integrating nonlinear models of the soleus muscle dynamics and account for delays in the reflex response dynamics.

## REFERENCES


Andersen, J. and Sinkjaer, T. (1995). An actuator system for investigating electrophysiological and biomechanical features around the human ankle joint during gait. *IEEE Transactions on Rehabilitation Engineering*, 3, 299–306. doi:10.1109/86.481969.

Downey, R.J., Cheng, T.H., Bellman, M.J., and Dixon, W.E. (2017). Switched tracking control of the lower limb during asynchronous neuromuscular electrical stimulation: Theory and experiments. *IEEE Transactions on Cybernetics*, 47(5), 1251–1262. doi: 10.1109/TCYB.2016.2543699.

Filippov, A.F. (1964). Differential equations with discontinuous right-hand side. In *Fifteen papers on differential equations*, volume 42 of *American Mathematical Society Translations - Series 2*, 199–231. American Mathematical Society.

Fischer, N., Kamalapurkar, R., and Dixon, W.E. (2013). LaSalle-Yoshizawa corollaries for nonsmooth systems. *IEEE Transactions on Automatic Control*, 58(9), 2333–2338. doi:10.1109/TAC.2013.2246900.

Gandolla, M., Guanziroli, E., D'Angelo, A., Cannaviello, G., Molteni, F., and Pedrocchi, A. (2018). Automatic setting procedure for exoskeleton-assisted overground gait: Proof of concept on stroke population. *Frontiers in Neurorobotics*, 12(MAR). doi:10.3389/fnbot.2018.00010.

Gottlieb, G.L. and Agarwal, G.C. (1979). Response to sudden torques about ankle in man: myotatic reflex. *Journal of Neurophysiology*, 91–106.

H. K. Khalil (2002). *Nonlinear Systems*. Prentice Hall, 3 edition.

Hornby, T.G., Reisman, D.S., Ward, I.G., Scheets, P.L., Miller, A., Haddad, D., Fox, E.J., Fritz, N.E., Hawkins, K., Henderson, C.E., Hendron, K.L., Holleran, C.L., Lynskey, J.E., and Walter, A. (2020). *Clinical Practice Guideline to Improve Locomotor Func-*

*tion Following Chronic Stroke, Incomplete Spinal Cord Injury, and Brain Injury*, volume 44. doi: 10.1097/NPT.0000000000000303.

Krstić, M., Kanellakopoulos, I., and Kokotović, P. (1995). *Nonlinear and Adaptive Control Design*. Wiley.

Kulmala, J., Korhonen, M., Ruggiero, L., Kuitunen, S., Suominen, H., Heinonen, A., Mikkola, A., and Avela, J. (2016). Walking and Running Require Greater Effort from the Ankle than the Knee Extensor Muscles. *Medicine and Science in Sports and Exercise*, 48, 2181–2189. doi:10.1249/MSS.0000000000001020.

Lipfert, S., Gunther, M., Renjewski, D., and Seyfarth, A. (2014). Impulsive ankle push-off powers leg swing in human walking. *Journal of Experimental Biology*, 217, 1831–1831. doi:10.1242/jeb.107391.

Marchal-Crespo, L. and Reinkensmeyer, D.J. (2009). Review of control strategies for robotic movement training after neurologic injury. *Journal of NeuroEngineering and Rehabilitation*, 6(1). doi:10.1186/1743-0003-6-20.

Mazzaro, N., Grey, M.J., and Sinkjær, T. (2005). Contribution of afferent feedback to the soleus muscle activity during human locomotion. *Journal of Neurophysiology*, 93(1), 167–177. doi:10.1152/jn.00283.2004.

Perreault, E.J., Crago, P.E., and Kirsch, R.F. (2000). Estimation of intrinsic and reflex contributions to muscle dynamics: a modeling study. *IEEE Transactions on Biomedical Engineering*, 1413–1421. doi: 10.1109/TBME.2000.880092.

Riener, R., Ferrarin, M., Pavan, E.E., and Frigo, C.A. (2000). Patient-driven control of FES-supported standing up and sitting down: Experimental results. *IEEE Transactions on Rehabilitation Engineering*, 8(4), 523–529. doi:10.1109/86.895956.

Schauer, T., Negård, N.O., Previdi, F., Hunt, K.J., Fraser, M.H., Ferchland, E., and Raisch, J. (2005). Online identification and nonlinear control of the electrically stimulated quadriceps muscle. *Control Engineering Practice*, 13(9), 1207–1219. doi: 10.1016/j.conengprac.2004.10.006.

Weerdesteyn, V., De Niet, M., Van Duijnhoven, H.J., and Geurts, A.C. (2008). Falls in individuals with stroke. *Journal of Rehabilitation Research and Development*, 45(8), 1195–1214. doi:10.1682/JRRD.2007.09.0145.

Winter, D.A. (2009). *Biomechanics and Motor Control of Human Movement: Fourth Edition*. New York: Wiley. doi:10.1002/9780470549148.

Yang, J., Stein, R., and James, K. (1991). Contribution of peripheral afferents to the activation of the soleus muscle during walking in humans. *Experimental Brain Research*, 87, 1373–1383. doi:10.1007/BF00227094.